Synthesis and Characterization of Macroporous Thermosensitive Hydrogels from Recombinant Elastin-Like Polymers

Laura Martín, Matilde Alonso, Alessandra Girotti, F. Javier Arias, and J. Carlos Rodríguez-Cabello*

Multifunctional bioactive chemically cross-linked elastin-like polymers (ELPs) have been prepared as three-dimensional scaffolds for tissue engineering. The salt-leaching/gas-foaming technique was found suitable to prepare highly porous biodegradable hydrogels based on this novel material type. The porosity can be controlled by the amount of sodium hydrogen carbonate incorporated during the cross-linking reaction, whereas the mean pore size is determined by the salt particle size. The gas-foaming process, which involves immersion in a citric acid solution after the cross-linking, facilitates pore interconnectivity and allows a grooved surface essential for cell colonization. Due to the thermoresponsive nature of the ELPs, their physical properties are strongly influenced by the temperature of the aqueous medium. The feasibility to obtain tridimensional scaffolds for tissue engineering has been studied by testing the adhesion and spreading of endothelial cells into the porous ELP hydrogels. The methods and structures described herein provide a starting point for the design and synthesis of macroporous multifunctional elastin-like hydrogels with potential broad applicability.

Introduction

Researchers in the field of tissue engineering are continually searching for materials with additional tissue-specific properties or which could be tailored to several tissue systems. The scaffold composition may include desirable properties such as specific interactions with extracellular matrix components, growth factors or cell-surface receptors. A great deal of interest is currently being focused on new classes of biodegradable polymers with specific or controllable bioactivity. The extracellular matrix (ECM) is a composite material which contains a complex mixture of fibrous proteins and heteropolysaccharides and provides an important model for the design of biomaterials.[1,2] Modern genetic engineering techniques allow the design and expression of artificial genes to prepare proteinaceous analogues of ECM proteins with controlled mechanical properties, and which incorporate domains that modulate cellular behavior.[3−6] The goal of mimicking the ECM's structure and biological functions requires the design of artificial scaffolds that reproduce one or, preferably, more of the properties and functionalities of the natural tissue.

One of the most important examples of this new generation of ECM-mimicking materials is the family of recombinant elastin-like polymers (ELPs). They are inspired by the amino acid sequence of native elastin, one of the most abundant ECM proteins. In its natural state, elastin is an insoluble protein due to the presence of cross-links. However, its soluble forms, such as tropoelastin[7] or α-elastin,[8] are frequently used as biomaterials. In both cases, although more evident for ELPs, biotechnological techniques have been exploited to create tailored protein polymers with programmable sequences. This allows highly complex ELPs containing structural and functional domains derived from different ECM proteins to be obtained with total control of the molecular architecture. These biomimicking biopolymers can include cell-binding peptides such as RGD, REDV, and so on, which are sequences that promote specific cellular responses by mediating cell adhesion via integrins.[9−11] The ELP family of polymers shows a wide range of interesting properties that are rarely found together in any other polymeric material, namely, biocompatibility, mechanical properties (similar to those of natural ECM), a stimuli-responsive nature, and self-assembly behavior, and the obvious possibility of incorporating any function derived from peptidic domains into their composition. The most peculiar property of these polymers, however, is probably their stimuli-responsive behavior. ELPs undergo a phase transition in response to temperature changes. Below a critical temperature, known as the transition temperature (T_t), the un-cross-linked polymer chains are soluble in water, whereas above T_t the polymer chains form nano- and micro-aggregates, which separate from solution.[3,12] An understanding of the molecular basis of this stimuli-responsive behavior has opened up the opportunity to create ELPs that respond, under isothermal conditions, to a number of external stimuli, including light, redox changes, pH, concentration of diverse analytes, and pressure, by exploiting the so-called ΔT_t and amplified ΔT_t mechanisms.[13−15]

The enormous potential of this kind of protein polymer as a truly advanced material for a variety of biomedical applications, ranging from scaffolds for tissue engineering and regenerative medicine to cell-based microdevices, has boosted the exploration of the different ways that these peculiar polymers can be processed to achieve practical scaffolds and systems for use in different contexts, thereby showing the potential to improve the currently existing alternatives. In this regard, ELP scaffolds have been produced in the form of electrospun fibers,[16] hybrid hydrogels[17] and 2D films,[18] and ELP hydrogels have been produced by photoinitiation,[19] irradiation,[20,21] amine reactivity,[22−26] and enzymatic cross-linking by tissue transglutaminase.[27] However, due to the short history of this family and the fact that these materials are not commercially available, a great deal

of fundamental knowledge regarding their properties is still lacking. For example, although ELP hydrogels with different compositions have been tested in terms of bioactivity, swelling ratio, or mechanical properties, their microstructure, which is very important for tissue engineering applications, has not been studied in-depth. One of the most obvious knowledge gaps for ELP hydrogels is that few studies concerning the possibility of obtaining suitable macroporous scaffold structures for subsequent use in 3D cell culture procedures have been performed.

Three-dimensional polymer scaffolds provide a suitable space in which transplanted cells can grow and generate their own extracellular matrix. This artificial scaffold should ideally degrade into nontoxic components that can be eliminated or reabsorbed from the implant site. A high porosity is required to offer sufficient space for tissue ingrowth and to improve the invasion of surrounding tissues. A well-defined pore size and interconnecting pore network are also essential for vascularization and nutrient diffusion. It is also desirable that these scaffolds are biocompatible, biodegradable, and exhibit appropriate mechanical properties if required for the application and manufacturing technique to be used.[28,29] Several methods have been used to obtain these kinds of porous scaffolds from biodegradable materials, including solvent casting/porogen leaching,[30,31] gas foaming with pressurized carbon dioxide,[8,32] electrospinning,[33,34] emulsion freeze-drying,[35,36] 3D printing,[37,38] salt leaching/gas foaming,[39,40] and, more recently, combinations of these methods. These techniques have been used with both natural (gelatin, chitosan or alginate) and synthetic biodegradable polymers such as polyesters, poly(vinyl alcohol), or poly(urethane)s, although their use with ELPs has not been reported.[1,41]

Due to the water solubility of most ELPs, many of the existing methods to create macroporous structures cannot be used. Among those methods that could be used, however, salt leaching is one of the most attractive. We have therefore evaluated the possibility of adapting current technology for this purpose. In this work, we adapt the standard salt-leaching/gas-foaming method to obtain appropriate bioactive scaffolds for 3D tissue engineering from ELPs. In general, the salt-leaching technique has shown, with other polymer systems, that porosity and pore size can be controlled by varying the amount of salt present and its particle size, respectively. The salt (usually NaCl) is incorporated during the cross-linking reaction with materials such as gelatin, poly-L-lactic acid (PLLA) or poly-DL-lactic-*co*-glycolic acid (PLGA), among others,[36,42] although it is difficult to obtain interconnected structures with this technique and the scaffolds often present a surface skin layer. It is possible to minimize these disadvantages of the salt-leaching technique by using the salt-leaching/gas-foaming method,[40] which is based on the idea that sieved particles of bicarbonate salts, dispersed within a polymer−solvent mixture, generate carbon dioxide gas in the matrix upon contact with hot water or acid solution, thereby producing highly porous scaffolds.

The pore size required depends on the type of cell to be grown on that scaffold and on the material. For example, a pore diameter of 100 μm and above is required to ensure a rich blood supply, nutrient delivery and gas exchange to promote the colonization of bone cells.[43,44] Pore-size control is therefore critical for controlling cellular colonization rates, angiogenesis, and organization within an engineered tissue. The pore morphology can also affect the scaffold degradation kinetics and the mechanical properties of the tissue significantly. In tissue engineering, scaffolds should supply mechanical support for the cellular microenvironment as well as transmit mechanical stimuli. Hydrogels are not simply elastic materials, but behave viscoelastically.[45−47] The viscoelastic properties correlate strongly with the microstructure and could provide useful information for tailoring their performance characteristics to suit given applications.

In this study, we present a simple method for preparing ELP-based macroporous hydrogels with tunable pore sizes and mechanical properties with the aim of gaining a fundamental understanding of how the introduction of salt particles affects the physical properties of thermally responsive ELP hydrogels. The reviewed literature suggests that there is no "ideal" scaffold for all tissue types, and we demonstrate herein that the physical properties of these materials can be tailored to future applications in tissue engineering and regenerative medicine by varying the size of the salt particles.[48,49] Furthermore, we have studied the influence of temperature on scaffolds made from stimuli-responsive ELPs. If this thermoresponsive behavior is found to remain in the cross-linked hydrogels, this could significantly broaden the potential of these biological systems for tissue-engineering purposes because, for example, their thermoresponsive nature could be exploited in combined drug-delivery and tissue-engineering strategies.

Experimental Section

Materials. The elastin-like polymer was biosynthesized and its biochemical and physical properties characterized by previously reported methods.[11] *N*,*N*-Dimethylformamide (DMF), dimethyl sulfoxide (DMSO), hexamethylene diisocyanate (HDI), sodium chloride (NaCl), sodium hydrogen carbonate ($NaHCO_3$), and anhydrous citric acid were purchased from Fluka Sigma-Aldrich (Madrid, Spain).

Salt particles were sieved in two different ranges [250−425 μm (A) and 180−250 μm (B)] before use.

Human umbilical vein endothelial cells (HUVECs; cat. no. cc-2517), endothelial growth medium (EGM; Clonetic, cat. no. cc-3124), serum-free culture medium (EBM Clonetics cat. no. cc-3121), accutase (cat. no. A6964 Sigma Aldric), DAPI (cat. no. PA-3013), Phalloidin-Alexa Fluor488 Conjugate (cat. no. PA-3010), and all other tissue culture reagents were purchased from Lonza. The remaining consumables for cell culture were obtained from Corning Inc. Costar.

Preparation of Porous ELP Hydrogels. The hydrogels were obtained by mixing a solution of the ELP (80 mg/mL) in DMSO/DMF (80:20) with an appropriate solution (25 mg/mL) of the homobifunctional cross-linker hexamethylene diisocyanate (HDI) in DMF in a polymer/cross-linker molar ratio of 1:3 at 4 °C. The mixture was stirred and poured into customized Teflon molds (Ø = 13.5 mm; h = 2 mm). Previously sieved NaCl or $NaHCO_3$ was added in a salt/polymer weight ratio of 10:1 or 20:1 and stirred to homogenize the sample. The reaction mixture was kept at room temperature for 3 h, then the salt-hydrogel samples incorporating $NaHCO_3$ were extracted from the mold and immersed in a 3 M citric acid solution for 45 min in an ultrasound bath. Finally, all the matrices were thoroughly washed with Milli-Q water to eliminate unreacted reagents and salts. Hydrogels prepared without porogen salts were used for reference.

Differential Scanning Calorimetry (DSC). The experiments were performed on a Mettler Toledo 822^e DSC with a liquid-nitrogen cooler, calibrated with a standard sample of indium. For analysis of the ELP, 20 μL of a 50 mg mL^{-1} polymer solution in Milli-Q water were placed in a 40 μL aluminum pan hermetically sealed. An equal volume of water was placed in the reference pan. For ELP-hydrogel analysis, 20 mg of the hydrated hydrogel was placed on the sample pan. To account for the exact amount of polymer in the assayed hydrogel, the sample was lyophilized and weighted after the DSC run. The heating program for both kinds of samples includes an initial isothermal stage (5 min at 0 °C) followed by heating at a constant rate of 5 °C min^{-1} from 0 to 50 °C.

Amino Acid Analysis. The amino acid composition was determined by the Technical-Scientific Service at the University of Barcelona

(Spain) by HCl hydrolysis, derivatization by the AccQ-Tag Waters method and subsequent analysis by HPLC with UV detection for quantification. Each sample has been analyzed by triplicate.

Physical Properties of ELP Hydrogels. The porosity of the hydrogels was determined in the swollen state in water using eq 1[50]

$$\text{porosity}(\%) = \left(\frac{W_1 - W_2}{d_{\text{water}}}\right) \times \frac{100}{V} \quad (1)$$

The swelling ratio (Q_w) of the hydrogels was estimated using eq 2

$$Q_w = \left(\frac{W_1}{W_2}\right) \quad (2)$$

where W_1 and W_2 are the weight of the swollen and lyophilized gel, respectively, d_{water} is the density of pure water, and $V(\Pi r^2 h)$ is the measured volume of the hydrogel in the swollen state. All measurements were taken 24 h after soaking the hydrogel in water at the appropriate temperature. Excess surface water was removed with a filter paper before each measurement.

Lyophilization or freeze-drying (FreeZone 1, LABCONCO) was performed from frozen hydrogels in liquid nitrogen previously swollen in water at the corresponding testing temperature.

Mechanical tests were performed on a strain-controlled rheometer (AR2000ex, TA Instruments) to measure the dynamic shear modulus (a measure of dynamic matrix stiffness). Swollen gels were placed between parallel plates (12 mm in diameter) and the gap adjusted starting from the sample to reach a normal force of about 0.3 N to prevent slippage. An amplitude sweep (storage modulus G' measured as a function of strain) was performed to confirm that the measurements were within the linear region of viscoelasticity. Measurements were then carried out in constant-strain mode (0.1%) as a function of frequency (from 0.1 to 10 Hz).

All physical properties mentioned above were measured at two testing temperatures: below (4 °C) and above (37 °C) T_t.

Microstructural Morphology. Freeze-dried ELP hydrogels were fractured after immersion in liquid nitrogen. The samples were coated with Au (Balzers-SCD 004) prior to SEM (JEOL, JSM-820) observation at 15.0 kV.

In addition, swollen hydrogels were heated from 4 to 37 °C and observed without sample preparation using environmental scanning electron microscopy (ESEM) (FEI Quanta 200FEG). The mean pore size was estimated using *Image J* software with at least 30 pores in three different spots for triplicate samples.

Statistical Analysis. Data are represented as the mean ± standard deviation (SD), $n = 3$. Statistical comparisons were performed by one-way ANOVA using Bonferroni corrected *t*-test with Graphpad Prism 4.0 software. A *p*-value of less than 0.05 was considered to be statistically significant (expressed in the figure with asterisks [*]: $*P < 0.05$; $**P < 0.01$; when present).

Cell Culture Assays. HUVECs were grown in EGM, which was replaced every two days, and were incubated at 37 °C in a 5% CO_2 humidified environmental chamber. Hydrogels for these cell culture assays were made with sodium hydrogen carbonate: polymer weight ratio of 20/1 using particles in the 180−250 μm size range. They were sterilized for cell culture by UV exposure overnight and stored in 70% ethanol. Before use, they were washed with sterile Milli-Q water, lyophilized, and placed in a 24-well plate. Near confluence HUVECs (passages 3−5) were harvested by accutase treatment and then washed and resuspended in EBM, seeded at 10000 cells/cm^2 on dried ELP hydrogels, and incubated at 37 °C. EBM minimal medium was used to promote specific cell−scaffold interaction. A total of 48 h after cell seeding, the hydrogels were washed with PBS to remove nonadhered cells and then fixed.

Samples for phase-contrast and epifluorescence were fixed in 4% paraformaldehyde for 10 min, permeabilized with 0.2% Triton X-100, and stained with the fluorescent dyes Phalloidin-Alexa Fluor488R and DAPI, as indicated in the text. The samples were observed by phase-contrast and fluorescence microscopy using a Nikon Eclipse Ti inverted microscope (Nikon Instruments/Europe) at a magnification of 10−20−40×.

Hydrogels seeded with cells for SEM analysis were fixed in Palay fixative[37] (1% gluteraldehyde and paraformaldehyde in 0.1 N calcium chloride solution) at pH 7.4 for 2 h at room temperature. Samples were progressively dehydrated in ethanol solutions (15, 30, 50, 70, 90, and, three times, 100%).

((VPGIG)$_2$VPGKG(VPGIG)$_2$EEIQIGHIPREDVDYHLYP(VPGIG)$_2$VPGKG(VPGIG)$_2$(VGVAPG)$_2$)$_{10}$

Figure 1. Scheme of the peptide domains and amino acid sequence of the designed polymer.

Results and Discussion

Cross-Linked Hydrogels and Thermal Behavior. The bioactive protein polymer used in this work was designed to be employed in tissue engineering with peptide sequences that provide an appropriate balance of bioactivity (cell adhesion sequence and specific biodegradability) and other functionalities (cross-linking domains and mechanical properties).[11] The monomer unit contains four different functional blocks (Figure 1). Thus, the $(VPGIG)_n$ sequence confers elasticity, biocompatibility, and thermoresponsive nature.[12] Some of the elastic domains have been modified to include lysines for cross-linking purposes and other potential chemical modifications while retaining the ELP properties. The next block contains periodically spaced fibronectin CS5 domains enclosing the cell attachment sequence REDV, which has been found to be specific for endothelial cells.[9] Finally, a target hexapeptide sequence for elastase-proteolitic action with bioactive properties (modulation of proliferation and migration among others) has been introduced.

Polymer cross-linking was performed by forming covalent links between the homobifunctional cross-linker HDI and the ε-amine groups of the polymer lysines in the organic solvent mixture described above. The cross-linking ratio (polymer/cross-linker 1:3) was selected to obtain hydrogels with optimal consistency and transparency (data not shown). To decrease the solution freezing point, a mixture of DMSO and DMF was chosen. Both solutions were stored at low temperature (4 °C) before mixing to decrease the cross-linker reactivity during the initial mixing and molding stages.

The inverse temperature transition (ITT) can be characterized by T_t and the enthalpy involved in the phase transition. Cross-linked ELP hydrogels prepared in the absence of salt particles retain the thermoresponsiveness characteristics of the ELPs displaying T_t (Figure 2). T_t is lower for the ELP hydrogel than for the free ELP. This was expected as the reaction of the ε-amine groups for cross-linkings causes a decrease in the mean polarity, which according to the literature is always accompanied by a decrease in T_t.[12] The enthalpy of the transition found in the hydrogel is slightly lower than the one found for the uncross-linked polymer. Although, in principle, the decrease in T_t should be accompanied by an increase in the enthalpy,[12] the dense cross-linked network leads to a decrease in chain mobility and partial loss of the conformational freedom. That would hinder the chain folding that takes place as an ELP is heated above its T_t, which could explain the relatively low value found for the enthalpy. Furthermore, there is a substantial broadening in the

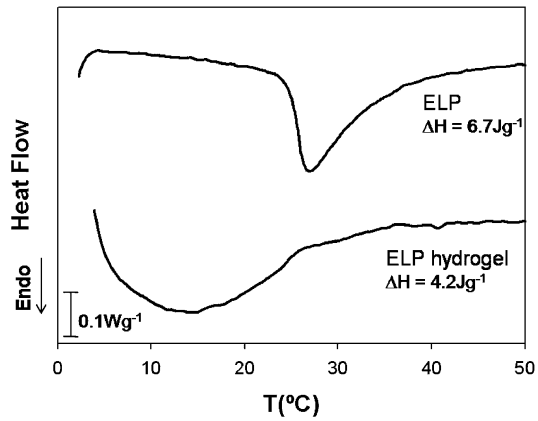

Figure 2. DSC thermograms of the ELP and the ELP-hydrogel at heating rate of 5 °C min $^{-1}$. The enthalpy of the phase transition is shown on the plot.

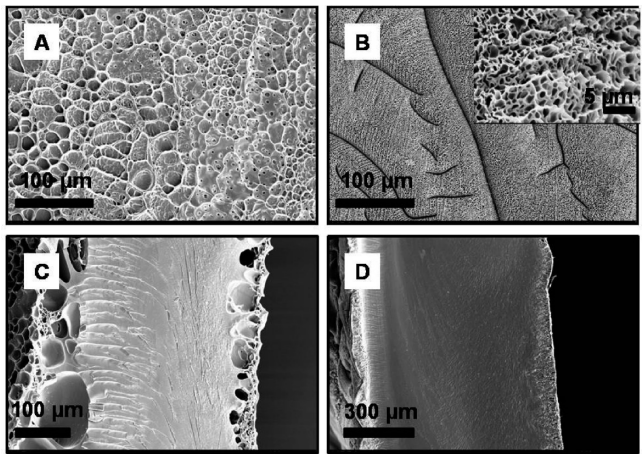

Figure 3. Swelling behavior and SEM micrographs of elastin-like hydrogels cross-linked in the absence of salt particles. Surface views: (A) 4 °C, (B) 37 °C; and cross sections: (C) 4 °C and (D) 37 °C.

endotherm, caused also by the hindered chain mobility, which plays an additional kinetic effect.

Cross-linked ELP hydrogels were first prepared in the absence of salt particles. Those samples exhibited certain intrinsic microporosity, as can be seen from the SEM micrographs in Figure 3. However, this intrinsic porosity proved to be of no use for creating 3D scaffolds for tissue engineering. Inspection of these images reveals that the surface shows a closed-pore structure. The mean pore size at 4 °C is 29.0 ± 11.1 μm (Figure 3A) as the structure is completely expanded, whereas at 37 °C, above T_t, the hydrogel collapses, which results in a substantial decrease in the mean pore size (1.3 ± 0.4 μm; Figure 3B). In addition, there is no porous organization inside the lyophilized hydrogel obtained in the absence of porogen salts at both tested temperatures (Figure 3C,D). These results show that the matrix retains the thermoresponsive nature of the original ELP but that the pore size and internal structure in ELP hydrogels cross-linked without porogen salts would not be suitable for cell colonization.

These results clearly indicate the need to use suitable methodologies to enhance the porosity and mean pore size in order to obtain adequate macroporous hydrogels for 3D cell culture. A first option in this direction is the simple method of salt leaching (with sodium chloride). As an example on the possibilities of this approach, ELP hydrogels were prepared with sieved sodium chloride particles at the following conditions: polymer weight ratio of 10/1 and particle size in the range

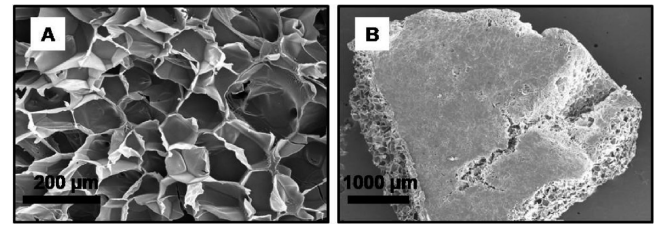

Figure 4. SEM micrographs of ELP hydrogels obtained by salt leaching: cross-sectional (A) and surface view (B).

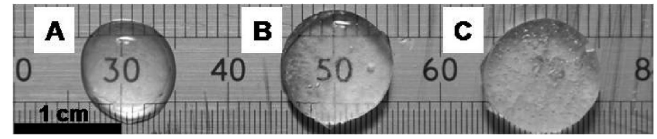

Figure 5. Macroscopic pictures of swollen hydrogels in water at 4 °C with different salt/polymer weight ratios: (A) 0/1, (B) 10/1, and (C) 20/1.

180−250 μm. The porous structure obtained is shown in Figure 4. SEM micrograph in Figure 4A demonstrates that it is possible to adapt this standard technique to ELPs to obtain homogeneous porous structures with a controlled pore size. However, this material contains no interconnected structures and the surface also exhibits a skin layer (Figure 4B). These results clearly show that this technique is suitable for obtaining macroporous scaffolds but that the interconnectivity still needs to be enhanced and the surface characteristics improved to allow cell colonization. The salt-leaching/gas-foaming method was therefore utilized to improve the properties of the hydrogels obtained using the salt-leaching method alone.

Morphological Characterization of Porous ELP Hydrogels Obtained by the Salt-Leaching/Gas-Foaming Method. Figure 5 shows macroscopic pictures of the swollen hydrogels. The hydrogel in Figure 5A was prepared in the absence of porogen salts, whereas the porous hydrogels shown in Figure 5B and C were prepared by the salt-leaching/gas-foaming method using increasing amounts of sodium hydrogen carbonate particles. As expected, the presence of pores clearly results in decreased gel transparency.

Amino acid analysis was used to study the degree of cross-linking; the results are summarized in Table 1. The degree of cross-linking can be determined from the content of free amino groups in the cross-linked hydrogels. This analysis clearly demonstrates the specific reactivity of HDI toward lysines in organic solvents as the content of other amino acids was not affected by the cross-linking reaction. The good specificity of HDI is of particular interest as undesirable specific reactions with possible reactive amino acids such as arginine (R), glutamic acid (E), or aspartic acid (D) involved in cell-adhesion induction could inhibit the bioactivity of the CS5 domain.[24] The presence of salt particles during the cross-linking reaction did not affect the degree of cross-linking significantly, with highly cross-linked hydrogels being obtained in all cases.

Scaffolds were prepared from sieved salt particles in two different size ranges: 180−250 and 250−425 μm. The scaffold pore morphology obtained with these two different size ranges was found to be retained in the hydrogel microstructures. The hydrogels show a uniform pore morphology with evenly distributed pores, as evidenced by the cross-sectional SEM micrographs (Figure 6), as was the case for the ELP hydrogels obtained using the salt-leaching method alone (Figure 4), thus, indicating that the salt type does not influence the pore organization inside the structure. The average pore size in the

Table 1. Amino Acid Analysis Comparing Theoretical and Experimental Results for Un-Cross-Linked ELP and Cross-Linked Hydrogels[a]

amino acid type	theoretical number of amino acids	experimental number for un-cross-linked ELP[11]	experimental number for hydrogels weight ratio salt/ polymer		
			0/1	10/1	20/1
Lys (K)	20	20.05	5.04 ± 0.03	4.04 ± 0.02	4.11 ± 0.04
Arg (R)	10	11.20	10.58 ± 0.01	10.84 ± 0.06	10.95 ± 0.04
Glx (E+Q)	41	42.13	39.67 ± 0.08	40.55 ± 0.20	40.87 ± 0.17
Asp (D)	20	20.41	21.34 ± 0.13	21.73 ± 0.06	21.81 ± 0.08
Val (V)	171	172.17	169.82 ± 0.27	170.98 ± 0.43	171.06 ± 0.73

[a] Data are reported as mean ± SD ($n = 3$).

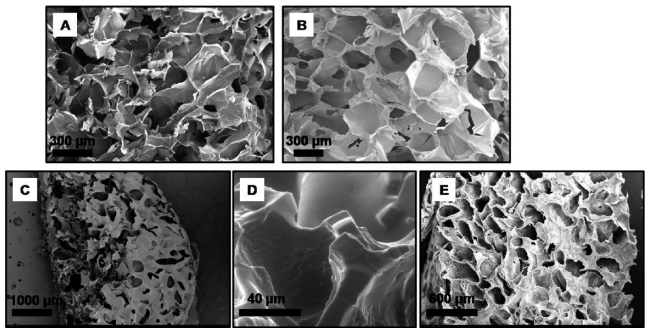

Figure 6. SEM micrographs of hydrogels obtained with different salt particle size ranges: (A) 180−250, (B) 250−425 μm. Surface views (C, D) and cross-sectional micrograph (E) of the 180−250 μm ELP hydrogels.

scaffolds was 208.6 ± 33.5 μm for materials obtained using salt particles in the range 180−250 μm (Figure 6A) and 318.7 ± 60.3 μm for materials obtained using particles in the 250−425 μm size range (Figure 6B). The pore-size distribution in the hydrogels is therefore in full agreement with the initial salt particle size-ranges. The interconnectivity between pores was found to be improved by the effervescent-ultrasound process, and macropores connected to adjacent pores via openings in the pore walls can be observed in the cross-sectional SEM micrographs shown in Figure 6A,B. The surface of these samples was found to be highly grooved and did not show any substantial formation of a skin layer, as can clearly be seen in Figure 6C. This feature differentiates our materials from many of the other hydrogels reported in the literature, including the ELP hydrogels mentioned above, where the existence of such a skin is quite a common feature. A magnified view of a surface pore in the hydrogel is shown in Figure 6D. This micrograph shows a pore wall thickness of a swollen hydrogel, which is about 15 μm. In addition to the macroporous structure induced by the salt particles, an intrinsic microporosity can still be observed in hydrogels at 37 °C, a temperature above T_t, which contributes to the enhanced structure roughness (Figure 6E) and could be important for promoting cell attachment.

Changes in the pore size of hydrogels immersed in water, due to the thermoresponsive behavior of ELPs, were observed by ESEM (Figure 7). A decrease in pore size of about 30% was observed for the same pores as the temperature was increased to above T_t. This responsive nature offers the possibility of changing the dimensions of the pore during the cell culture to study possible modifications in cell behavior. In any case, and for the pore sizes used in this work, the decrease in pore dimensions is not enough to compromise the possibility of cell infiltration as it will be later demonstrated in the cellular studies.

Effect of Salt Particle Size on Porosity. Porous hydrogels were prepared with two different salt particle ranges of sodium hydrogen carbonate to evaluate the dependence of porosity on the salt particle size. All hydrogels were synthesized by triplicate

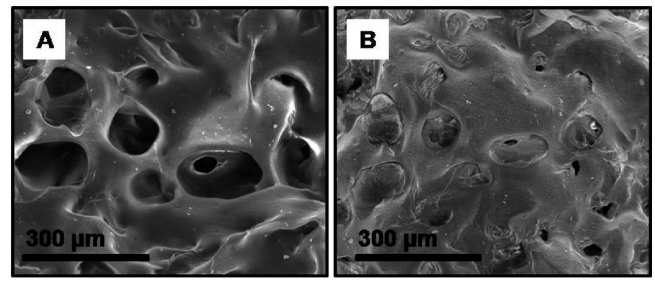

Figure 7. ESEM micrograph showing the change in pore size with temperature in swollen hydrogels: A, 4 °C; B, 37 °C.

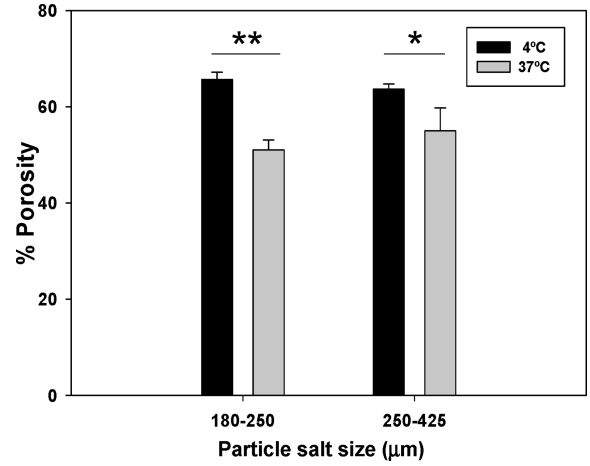

Figure 8. Effect of salt particle size and T_t on the porosity of hydrogels with a salt/polymer weight ratio of 10:1. Data are reported as mean ± SD ($n = 3$). Asterisk denotes significantly different p-values (*$P < 0.05$; **$P < 0.01$).

with a sodium hydrogen carbonate: polymer weight ratio of 10/1 and quantified using eq 1. In addition, the porosity of the swollen hydrogels was studied in water at two temperatures, one below (4 °C) and the other above (37 °C) T_t, to observe the influence of the temperature on the porosity.

The salt particles were sieved in the same ranges as above (180−250 and 250−425 μm). The results are plotted in Figure 8. The most obvious result is that porosity is influenced by temperature. The ELP hydrogels showed a porosity in the range 51−65% for the salt amount tested. The collapse above T_t due to the phase transition decreases the porosity significantly. Statistical analysis confirmed that there were no significant differences between the hydrogels obtained with different particle sizes at the same temperatures ($p > 0.05$) for similar amounts of salts. Hydrogels with similar porosity can therefore be prepared with different pore diameters simply by utilizing microsieved salt particles of different sizes.

Effect of the Salt/Polymer Weight Ratio on Porosity. Because porosity is not dependent on the salt particle size for equal salt amounts, hydrogels were prepared in triplicate with a salt particle size range of 180−250 μm, to study the influence of different salt amounts on the porosity. The hydrogels produced in the

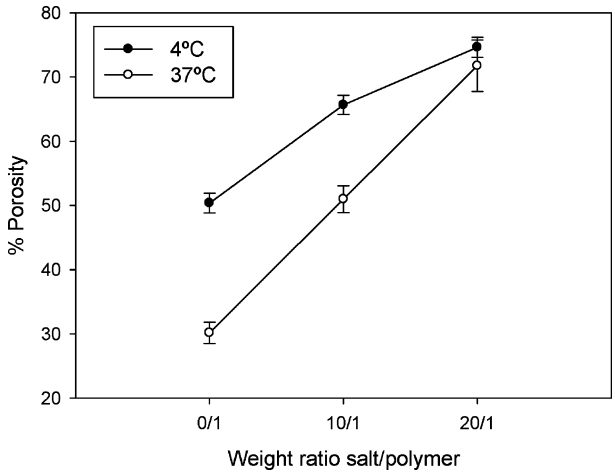

Figure 9. Influence of salt/polymer weight ratio on the porosity. SD indicated, $n = 3$.

Table 2. Swelling Ratio of Hydrogels Prepared with Sodium Hydrogen Carbonate (Size Range: 180−250 μm) in Water[a]

salt/polymer weight ratio	Q_w (4 °C)	Q_w (37 °C)
0/1	3.37 ± 1.10	1.70 ± 0.30
10/1	28.43 ± 3.63	2.61 ± 0.16
20/1	36.28 ± 1.63	10.10 ± 0.49

[a] Data are reported as mean ± SD ($n = 3$).

absence of salt porogens were used as reference; the porosity was calculated using Equation 1. Figure 9 shows the influence of the salt fraction on the porosity below (4 °C) and above T_t (37 °C). An increase in the salt/polymer ratio results in a high porosity of the cross-linked hydrogels under identical conditions, reaching as high as 75% at the highest salt amount tested in this work. Raising the temperature from 4 to 37 °C results in a decrease in the porosity, in agreement with the collapse previously observed in ELP hydrogels. Significant differences were found between samples with different salt/polymer ratios at the two testing temperatures except for hydrogels with high salt concentrations (20/1), which showed no significant differences in porosity with temperature.

Effect of Salt/Polymer Weight Ratio on Swelling. The swelling ratio was determined from eq 2 by soaking the hydrogels in Milli-Q water for 24 h. The results of this analysis are summarized in Table 2. The swelling ratio was found to increase significantly with an increase in the salt/polymer weight ratio. Thus, an increase in the salt/polymer weight ratio from 0/1 to 20/1 resulted in an increase in the swelling ratio (Q_w) from 3.37 ± 1.10 to 36.28 ± 1.63 at 4 °C. These results are in agreement with the increase in porosity. The swelling ratio decreases above T_t (37 °C) due to hydrogel collapse.

The phase transition of the ELP hydrogels can also be observed in the degree of swelling and contraction in aqueous solution and its dependence on temperature.

Effect of the Salt/Polymer Weight Ratio on the Rheological Properties. In general, hydrogels are viscoelastic materials. Their mechanical properties can be determined by rheological measurements in the linear viscoelastic range. Knowledge of the linear viscoelastic properties is of great importance since it allows to obtain information of the material in conditions close to unperturbed state. Therefore, in compliance with the principle of small deformation rheology,[46,47] the hydrogels must be tested within their respective linear viscoelastic ranges to ensure their stability. Samples were tested in their equilibrium swollen state completely immersed in a thermally regulated water bath during

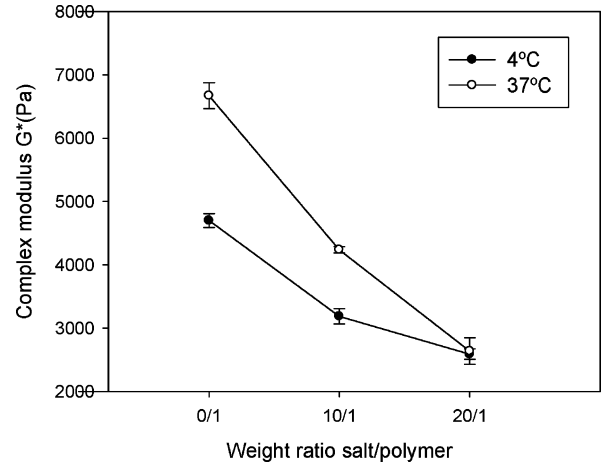

Figure 10. Influence of the salt/polymer weight ratio on the complex shear modulus. SD indicated, $n = 3$.

Table 3. Review of Physical Properties of Different Chemically Cross-Linkable ELP Hydrogels

cross-linker[a]	Q_w (H_2O Milli-Q)	mechanical evaluation	reference
HDI	3−36[b] 1.7−10[c]	G^* = 2.5−6.5 kPa	present study
HDI	0.37[b]	G = 0.13−0.31 MPa	25
TSAT	∼2−3.5[b] ∼0.2−0.6[c]	G^* = 1.6−15 kPa	26
THPP	12.3[b] 3.7[c]	G^* = 5.8−45.8 kPa	4

[a] Abbreviations: HDI, hexamethylene diisocyanate; TSAT, tris-succinimidyl aminotriacetate; THPP, tris(hydroxymethyl)phosphino-propionic acid. [b] Swelling temperature: 4 °C. [c] Swelling temperature: 37 °C.

the analysis, and a dynamic strain sweep was performed to determine the range of strain amplitudes for which ELP hydrogels exhibit that linear stress−strain behavior. Results confirmed that linear behavior was observed up to 0.3% strain, so that all subsequent tests were performed for a 0.1% strain. Thus, the dynamic shear modulus (a measure of dynamic matrix stiffness) was measured by frequency sweep tests between 0.1 and 10.0 Hz, showing a lineal behavior. The magnitudes of the dynamic shear modulus (G^*) are reported from data of a single frequency, 1.0 Hz, to compare among ELP hydrogels of varying salt amounts. Shear modulus (G^*) confirms that there is an inverse dependence between the mechanical properties and the porosity (Figure 10). The behavior below T_t confirms that the gel networks maintain contractile sensitivity to temperature changes. Raising the temperature from 4 to 37 °C, however, results in an increase in the elastic modulus with the salt/polymer weight ratio, thereby suggesting stiffer hydrogels at higher temperatures. Significant differences were found between samples with different salt/polymer ratios at both temperatures, except for those hydrogels with a high salt content (20/1). The thermal behavior of these hydrogels confirmed the results obtained on porosity (Figure 9) upon measuring the rheological properties.

The comparison with characterized cross-linked ELP hydrogels previously published in the literature allows to obtain a combined conclusion about their physical properties (Table 3). The swelling capacity of the ELP hydrogels fabricated in this study is considerable higher than other elastin-based hydrogels, because the addition of different salt amounts have substantial effect in the swelling behavior. The study of the dynamic shear modulus indicates that the type of cross-linker has an important effect, in addition to the cross-linking degree, which allows to

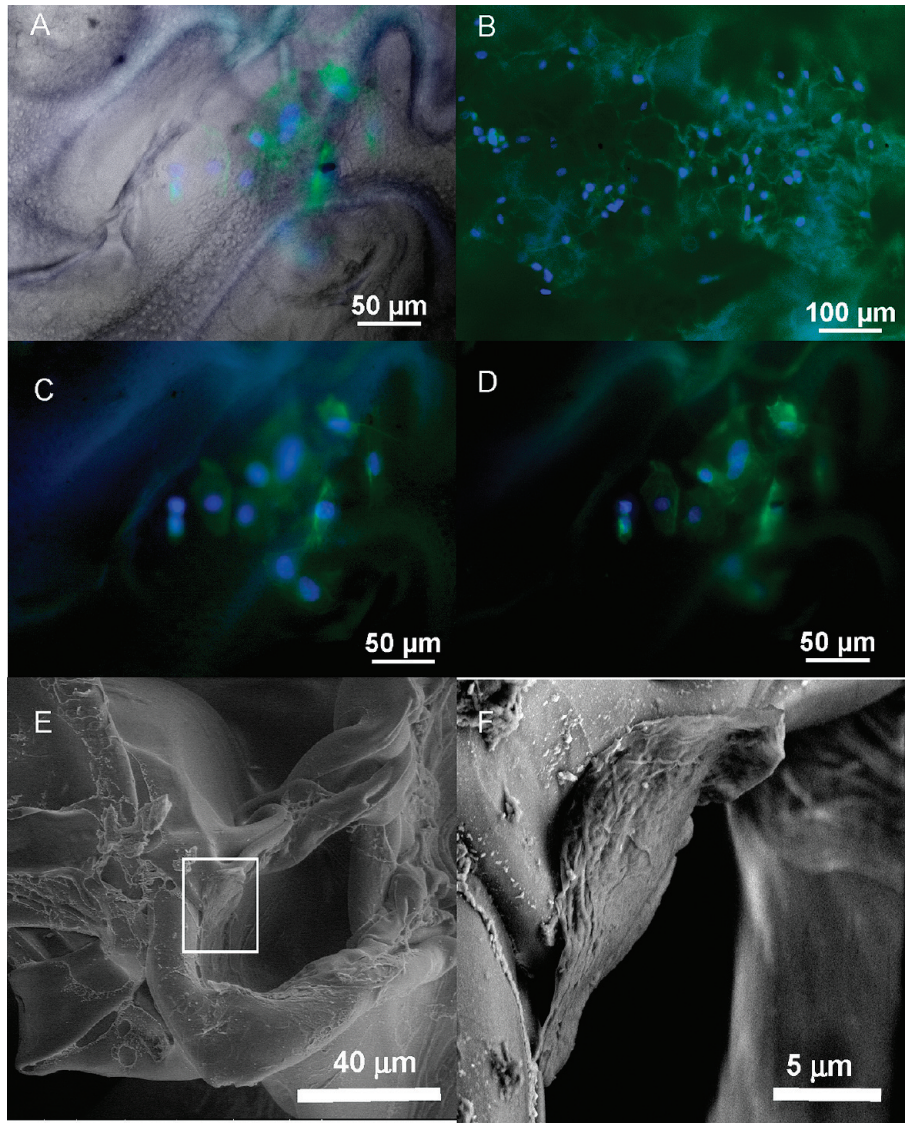

Figure 11. Microscopic captures and SEM micrographs of HUVECs seeded in macroporous ELP hydrogels after 48 h of incubation. Phase-contrast and fluorescence microscopy (A), fluorescence microscopy with Phalloidin Alexa Fluor488 and DAPI staining (B, C D). Cross-sectional SEM micrographs (E) and magnified view (F).

tune the mechanical properties. The reviewed literature confirms that there is not a study about the microstructure in hydrogels from ELPs.

Cell Viability and Morphology in Macroporous ELP Hydrogels. HUVECs have been shown selective binding and retention in REDV-coated surfaces[51] or REDV-ELP-coated surfaces.[22] Cell culture assays were performed to assess the suitability of 3-D REDV-containing scaffolds toward endothelial cells, in vitro. This last set of assays has two main goals. First, to test the biocompatibility of the scaffold in vitro and, second, that the open pore structure is suitable for cell infiltration. With the aim of promoting cell infiltration in the scaffold, the cells were seeded on lyophilized hydrogels to achieve quicker diffusion inside of matrices during the rehydration process. HUVECs viability and colonization of 3-D ELP hydrogel were evaluated by microscopy. Due to the transparency of the hydrogels, we were able to visualize by fluorescence microscopy the HUVECs integration in the scaffolds. As shown in Figure 11 numerous cells can be observed both in surface and inner layers of hydrogels situated in different focal planes testing that the cells were present in almost the totality of the hydrogel. This is specially evident in Figure 11C and D, where the same spot in the sample has been photographed at different depths. The macroporous structure of ELP hydrogels seems to offer a suitable environment for HUVECs that showed a well-spread morphology with large extensions, and their cytoskeleton actin filaments (green stained) were well organized in stress fibers (Figure 11C and D).

A cross-section of the cell-seeded ELP hydrogels was also analyzed by low vacuum SEM assays of cryo-fractured samples. Figure 11E,F shows the presence of cells within the internal pores.

Conclusions

A simple method for obtaining macroporous ELP hydrogels is reported in this work. Pore size can be controlled by varying the size of the salt particles incorporated during the cross-linking reaction. The results of this study demonstrate that the salt-leaching/gas-foaming technique can be used to synthesize chemically cross-linked highly porous ELP hydrogels with tunable physical properties. The use of gas-forming salts allows the formation of a highly interconnected porous structure, which is difficult to obtain in ELP hydrogels using more conventional

salt-leaching techniques. The porosity, swelling ratio, and mechanical properties have been shown to depend on the salt/polymer weight ratio and temperature. The thermal behavior of these materials has also been tested with respect to pore size and internal morphology. In addition to the macroporous structures resulting from the salt particles, these ELP hydrogels have also been shown to exhibit microporosity, which is intrinsic of these biomimetic materials.

In addition, we have demonstrated the feasibility of these ELP hydrogels to promote HUVECs adhesion and infiltration inside the porous structure of those matrices. This technique is therefore a straightforward approach to obtain advanced scaffolds with tunable biological and physical properties necessary for 3D cell culture. Bioactive, multifunctional ELP hydrogels have great potential for use as an artificial extracellular matrix in which the elasticity and thermoresponsive behavior of these materials could expand their range of potential applications.

Acknowledgment. We acknowledge financial support from the MICINN (Projects MAT 2007-66275-C02-01, NAN2004-08538, and PSE-300100-2006-1), the JCyL (Projects VA034A09, VA016B08, and VA030A08), the CIBER-BBN (Project CB06-01-0003), and the JCyL and the Instituto de Salud Carlos III under the "Network Center of Regenerative Medicine and Cellular Therapy of Castilla and León".

References and Notes

(1) Ma, P. X. *Adv. Drug Delivery Rev.* **2008**, *60*, 184–198.
(2) Badylak, S. F.; Freytes, D. O.; Gilbert, T. W. *Acta Biomater.* **2009**, *5*, 1–13.
(3) Rodríguez-Cabello, J. C.; Reguera, J.; Girotti, A.; Arias, F. J.; Alonso, M. *Adv. Polym. Sci.* **2006**, *200*, 119–167.
(4) Lim, D. W.; Nettles, D. L.; Setton, L. A.; Chilkoti, A. *Biomacromolecules* **2008**, *9*, 222–230.
(5) Huang, J.; Wong, C.; George, A.; Kaplan, D. L. *Biomaterials* **2007**, *28*, 2358–2367.
(6) Urry, D. W.; Pattanaik, A.; Xu, J.; Woods, T. C.; McPherson, D. T.; Parker, T. M. *J. Biomater. Sci., Polym. Ed.* **1998**, *9*, 1015–1048.
(7) Mithieux, S. M.; Rasko, J. E. J.; Weiss, A. S. *Biomaterials* **2004**, *25*, 4921–4927.
(8) Annabi, N.; Mithieux, S. M.; Weiss, A. S.; Dehghani, F. *Biomaterials* **2009**, *30*, 1–7.
(9) Mould, A. P.; Wheldon, L. A.; Komoriya, A.; Wayner, E. A.; Yamada, K. M.; Humphries, M. J. *J. Biol. Chem.* **1990**, *265*, 4020–4024.
(10) Hubbell, J. A.; Massia, S. P.; Desai, N. P.; Drumheller, P. D. *Biotechnology* **1991**, *9*, 568–572.
(11) Girotti, A.; Reguera, J.; Rodriguez-Cabello, J. C.; Arias, F. J.; Alonso, M.; Testera, A. M. *J. Mater. Sci.: Mater. Med.* **2004**, *15*, 479–484.
(12) Urry, D. W. *What sustains life? Consilient mechanisms for protein-based machines and materials*; Springer-Verlag: New York, 2006.
(13) Kostal, J.; Mulchandani, A.; Chen, W. *Macromolecules* **2001**, *34*, 2257–2261.
(14) Meyer, D. E.; Kong, G. A.; Dewhirst, M. W.; Zalutsky, M. R.; Chilkoti, A. *Cancer Res.* **2001**, *61*, 1548–1554.
(15) Rodríguez-Cabello, J. C.; Alonso, M.; Guiscardo, L.; Reboto, V.; Girotti, A. *Adv. Mater.* **2002**, *14*, 1151–1154.
(16) Huang, L.; McMillan, R. A.; Apkarian, R. P.; Pourdeyhimi, B.; Conticello, V. P.; Chaikof, E. L. *Macromolecules* **2000**, *33*, 2989–2997.
(17) Garcia, Y.; Hemantkumar, N.; Collighan, R.; Griffin, M.; Rodriguez-Cabello, J. C.; Pandit, A. *Tissue Eng., Part A* **2009**, *15*, 887–899.
(18) Liu, J. C.; Tirrell, D. A. *Biomacromolecules* **2008**, *9*, 2984–2988.
(19) Nagapudi, K.; Brinkman, W. T.; Leisen, J. E.; Huang, L.; McMillan, R. A.; Apkarian, R. P.; Conticello, V. P.; Chaikof, E. L. *Macromolecules* **2002**, *35*, 1730–1737.
(20) Lee, J.; Macosko, C. W.; Urry, D. W. *Macromolecules* **2001**, *34*, 5968–5974.
(21) Lee, J.; Macosko, C. W.; Urry, D. W. *Macromolecules* **2001**, *34*, 4114–4123.
(22) Heilshorn, S. C.; DiZio, K. A.; Welsh, E. R.; Tirrell, D. A. *Biomaterials* **2003**, *24*, 4245–4252.
(23) Lim, D. W.; Nettles, D. L.; Setton, L. A.; Chilkoti, A. *Biomacromolecules* **2007**, *8*, 1463–1470.
(24) Nowatzki, P. J.; Tirrell, D. A. *Biomaterials* **2004**, *25*, 1261–1267.
(25) Di Zio, K.; Tirrell, D. A. *Macromolecules* **2003**, *36*, 1553–1558.
(26) Trabbic-Carlson, K.; Setton, L. A.; Chilkoti, A. *Biomacromolecules* **2003**, *4*, 572–580.
(27) McHale, M. K.; Setton, L. A.; Chilkoti, A. *Tissue Eng.* **2005**, *11*, 1768–1779.
(28) Chen, G. P.; Ushida, T.; Tateishi, T. *Macromol. Biosci.* **2002**, *2*, 67–77.
(29) Weigel, T.; Schinkel, G.; Lendlein, A. *Expert Rev. Med. Dev.* **2006**, *3*, 835–851.
(30) Mikos, A. G.; Thorsen, A. J.; Czerwonka, L. A.; Bao, Y.; Langer, R.; Winslow, D. N.; Vacanti, J. P. *Polymer* **1994**, *35*, 1068–1077.
(31) Barbanti, S. H.; Zavaglia, C. A. C.; Duek, E. A. D. *Mater. Res.* **2008**, *11*, 75–80.
(32) Sheridan, M. H.; Shea, L. D.; Peters, M. C.; Mooney, D. J. Bioadsorbable polymer scaffolds for tissue engineering capable of sustained growth factor delivery. *5th Symposium on Controlled Drug Delivery*, Noordwijk Aan Zee, Netherlands, Apr 01−03, 1998; Noordwijk Aan Zee: Netherlands, 1998; pp 91−102.
(33) Zhao, L.; He, C. G.; Gao, Y. J.; Cen, L.; Cui, L.; Cao, Y. L. *J. Biomed. Mater. Res.* **2008**, *87B*, 26–34.
(34) Kim, T. G.; Chung, H. J.; Park, T. G. *Acta Biomater.* **2008**, *4*, 1611–1619.
(35) Sultana, N.; Wang, M. *J. Mater. Sci.: Mater. Med.* **2008**, *19*, 2555–2561.
(36) Kang, H. W.; Tabata, Y.; Ikada, Y. *Biomaterials* **1999**, *20*, 1339–1344.
(37) Liu, C. Z.; Xia, Z. D.; Han, Z. W.; Hulley, P. A.; Triffitt, J. T.; Czernuszka, J. T. *J. Biomed. Mater. Res.* **2008**, *85B*, 519–528.
(38) Lee, K. W.; Wang, S. F.; Lu, L. C.; Jabbari, E.; Currier, B. L.; Yaszemski, M. J. *Tissue Eng.* **2006**, *12*, 2801–2811.
(39) Nam, Y. S.; Yoon, J. J.; Park, T. G. *J. Biomed. Mater. Res.* **2000**, *53*, 1–7.
(40) Wachiralarpphaithoon, C.; Iwasaki, Y.; Akiyoshi, K. *Biomaterials* **2007**, *28*, 984–993.
(41) Nair, L. S.; Laurencin, C. T. *Prog. Polym. Sci.* **2007**, *32*, 762–798.
(42) Tsioptsias, C.; Tsivintzelis, I.; Papadopoulou, L.; Pallayiotou, C. *Mater. Sci. Eng., C* **2009**, *29*, 159–164.
(43) Roach, P.; Eglin, D.; Rohde, K.; Perry, C. C. *J. Mater. Sci.: Mater. Med.* **2007**, *18*, 1263–1277.
(44) Freyman, T. M.; Yannas, I. V.; Gibson, L. J. *Prog. Mater. Sci.* **2001**, *46*, 273–282.
(45) Anseth, K. S.; Bowman, C. N.; BrannonPeppas, L. *Biomaterials* **1996**, *17*, 1647–1657.
(46) Meyvis, T. K. L.; Stubbe, B. G.; Van Steenbergen, M. J.; Hennink, W. E.; De Smedt, S. C.; Demeester, J. *Int. J. Pharm.* **2002**, *244*, 163–168.
(47) Kavanagh, G. M.; Ross-Murphy, S. B. *Prog. Polym. Sci.* **1998**, *23*, 533–562.
(48) Rehfeldt, F.; Engler, A. J.; Eckhardt, A.; Ahmed, F.; Discher, D. E. *Adv. Drug Delivery Rev.* **2007**, *59*, 1329–1339.
(49) Discher, D. E.; Janmey, P.; Wang, Y. L. *Science* **2005**, *310*, 1139–1143.
(50) Zeng, X. F.; Ruckenstein, E. *Ind. Eng. Chem. Res.* **1996**, *35*, 4169–4175.
(51) Plouffe, B. D.; Njoka, D. N.; Harris, J.; Liao, J.; Horick, N. K.; Radisic, M.; Murthy, S. K. *Langmuir* **2007**, *23*, 5050–5055.

BM900560A